LIMNOLOGY
and
OCEANOGRAPHY

ASLO

Limnol. Oceanogr. 00, 2015, 00–00

doi: 10.1002/lno.10118

Methane transport through submarine groundwater discharge to the North Pacific and Arctic Ocean at two Alaskan sites

Alanna L Lecher,*[1] John Kessler,[2] Katy Sparrow,[2] Fenix Garcia-Tigreros Kodovska,[2] Natasha Dimova,[3,4] Joseph Murray,[5] Slawek Tulaczyk,[1] Adina Paytan[1,3,5]

[1]Department of Earth and Planetary Sciences, University of California Santa Cruz, Santa Cruz, California
[2]Department of Earth and Environmental Sciences, University of Rochester, Rochester, New York
[3]Institute of Marine Sciences, University of California Santa Cruz, Santa Cruz, California
[4]Department of Geological Sciences, University of Alabama, Tuscaloosa, Alabama
[5]Department of Ocean Sciences, University of California Santa Cruz, Santa Cruz, California

Abstract

Here, we quantify the flux of methane to the coastal Arctic and North Pacific Oceans via submarine groundwater discharge (SGD), by use of naturally occurring radium isotopes as groundwater tracers, combined with methane concentration measurements of coastal groundwater. Our findings indicate the flux of methane through this process is much greater in the coastal North Pacific (35 ± 27 mg m^{-1} d^{-1}) than the Arctic Ocean (4.1 ± 0.6 to 11.8 ± 3.9 mg m^{-1} d^{-1}). The dominant controls on methane flux through SGD were not methane concentrations in the aquifer but rather the hydrologic characteristics of each site that mitigated or intensified the SGD water volume flux (120 ± 50 m^3 m^{-1} d^{-1} in the North Pacific compared to 12 ± 4 m^3 m^{-1} d^{-1} in the Arctic). Tidal pumping was observed to be an especially important control on SGD flux at the North Pacific site.

Recent studies have noted the importance of the coastal high-latitude ocean to the global atmospheric methane budget (Shakhova et al. 2009). Super-saturation of methane has been found in high latitude coastal ocean areas, such as the East Siberian Shelf (Shakhova et al. 2010). Several sources of methane have been recognized including gas hydrate dissociation, submarine permafrost melt, and diffusion from shallow submarine sediments (Hovland et al. 1993; Archer et al. 2009; Overduin et al. 2012). However, the observed enrichment of methane in the high-latitude coastal ocean could also be attributed in part to a conduit that transports methane from the continent to the ocean, such as submarine groundwater discharge (SGD).

SGD is a mixture of fresh groundwater and seawater that has recirculated through the subterranean estuary (STE) as a result of tides and wave action which discharges to the ocean (Moore 1999). The STE is a reaction zone where fresh groundwater and seawater mix in the coastal porous substrate, and where mixing induced chemical reactions occur (Moore 1999). In this study, we define groundwater as any fluid (seawater, fresh groundwater, or mixture of the two) within the saturated zone of the STE, and coastal groundwater as specifically groundwater collected from the beaches of the study sites. SGD has consistently been implicated as a source of nutrients and other constituents to the coastal ocean (Knee and Paytan 2011 and refernces therein). There is evidence that SGD can be enriched in methane (Bugna et al. 1996; Cable et al. 1996; Dulaiova et al. 2010), and can act as a conduit for methane input into lakes in Arctic environments (Paytan et al. 2015). However, no studies have investigated methane in SGD in the coastal ocean at high latitudes.

Radium (Ra) isotopes have been used for almost 20 yr to detect and quantify SGD, coastal mixing, and transformations within the STE (Moore 1996, 2008). Radium isotopes are the decay products of the U/Th decay series (^{223}Ra from ^{235}U and ^{224}Ra and ^{228}Ra from ^{232}Th) that occur naturally in many of the earth's crustal materials. At high ionic strength such as in brackish waters, radium desorbs from aquifer materials, causing coastal aquifers which are inundated with seawater to be enriched in radium isotopes (Moore and Krest 2004). When groundwater discharges from the coastal aquifer to the ocean, the radium isotopes are transported with the groundwater, and they can be measured to quantify SGD, and the flux of constituents associated with SGD (Knee and Paytan 2011). The goal of this study is to use radium isotopes to quantify methane fluxes to the coastal ocean

*Correspondence: alecher@ucsc.edu

through SGD along the North Pacific and Arctic coastlines of Alaska.

Alaska is of particular interest to this study, because super-saturation of methane was found in East Siberian shelf waters and the Northwest passage (Shakhova and Semiletov 2007; Kitidis et al. 2010). The organic rich soils of the active layer above the permafrost of northern Alaska are prime substrates for methane production (Zimov et al. 2006). Melting of permafrost further releases organic material into the active layer, which increases methane production (Zimov et al. 2006). Furthermore, methane-producing coal deposits in southern Alaska (most-notably the Kenai Peninsula) contribute methane to aquifers in southern Alaska (Flores and Stricker 1992). This methane could be transported via SGD to coastal waters surrounding Alaska (Fig. 1).

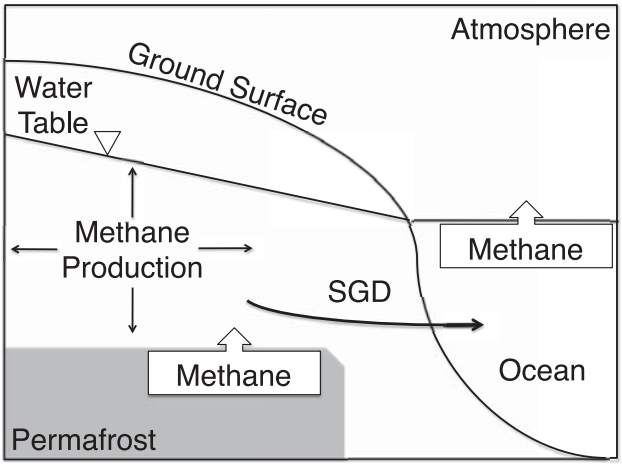

Fig. 1. A conceptual model of methane transport through SGD. Methane enters the coastal aquifer through melting of permafrost and biological processes. Methane-enriched groundwater then discharge to the ocean, where methane can degas to the atmosphere.

Methods

Study sites

Two study sites were chosen to represent contrasting permafrost and hydrologic regimes on the northern and southern coasts of Alaska (Fig. 2). Kasitsna Bay is a spit-enclosed inlet located in Katchemak Bay, an offshoot of the Cook Inlet on the southern coast of Alaska. It is approximately 1 km wide with a maximum depth of 58 m, but most of the bay having a depth in the range of 3–30 m. The bay is subject to a large tidal range (> 8 m) and the Kenai Peninsula, bordering the bay, is subject to high mean annual precipitation (450–800 mm) and is characterized by high topographic relief (Boucher and Mead 2006). These hydrologic characteristics are conducive to high rates of groundwater flow by tidal pumping and a steep hydraulic gradient. Permafrost coverage on the Kenai Peninsula is sporadic (< 5% coverage) (Brown et al. 2001).

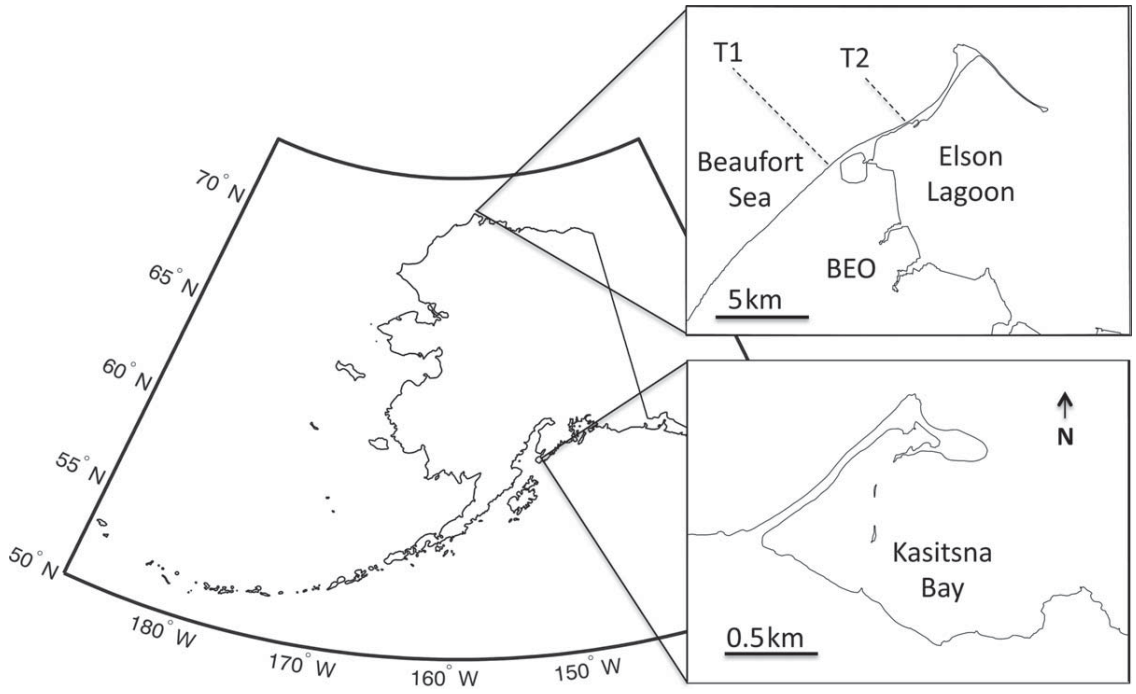

Fig. 2. A map of the study sites in Alaska. Elson Lagoon and Kasitsna Bay are well defined by the spits that enclose them. The area of study in the Beaufort Sea is confined to within 0.5 km of shore. Dashed lines represent two transects, transect 1 (T1) an transect two (T2) which a reperpendicular to shore.

Elson Lagoon is a spit-enclosed inlet located on the North Slope of Alaska. It is approximately 10 km wide and 20 km long, with an average depth of <3 m. Across the spit enclosing Elson Lagoon is the Beaufort Sea (Fig. 2), which was also sampled. Sampling of the Beaufort Sea extended along a 5 km length of coastline and up to 10 km from shore. The Beaufort Sea and Elson Lagoon are subject to small tidal ranges ($<$ 0.2 m). The adjacent coastal tundra has a low topographic relief and a mean annual precipitation of only 114 mm (Stafford et al. 2000). These hydrologic characteristics are not especially conducive to high SGD fluxes. Permafrost coverage of the coastal tundra on the North Slope of Alaska is continuous ($>$ 95% coverage) and at Point Barrow extends beneath the continental shelf offshore (Brown et al. 2001; Overduin et al. 2012). The permafrost laden soil on land at Barrow is composed of gleyed, sticky soil which underlies a water logged soil layer, and the mineral soil is either lacustrine or marine sediments. (Hinkel and Nelson 2003; Munroe et al. 2007). The depth of the active layer in these soils ranges from 30 cm to 60 cm with an average of 35 cm. Beach faces at all sites generally consisted of well-sorted gravel, with small ungauged rivers and creeks flowing into the Kasitsna Bay and Elson Lagoon study areas.

General sampling methods

Discrete seawater, groundwater, and river water samples were collected from Kasitsna Bay in August 2011 and July 2012 and the Beaufort Sea and Elson Lagoon in August 2012. Kasitsna Bay and Elson Lagoon are semienclosed by a spit, and seawater samples were collected along the shoreline and from the interior of the bay/lagoon. Samples were collected from the surface in both locations, and some additional samples were collected from a depth of 18 m at Kasitsna Bay. At the Beaufort Sea seawater samples were collected along 5 km of the coast (half of which was located along the spit enclosing the lagoon) and along two transects extending perpendicular from the coast up to 10 km offshore. Groundwater samples were collected in all locations from freshly dug pits or temporary PVC well points of variable depth depending on the depth of the water table. In 2011, groundwater samples were also collected from five private fresh drinking wells in the area surrounding Kasitsna Bay; these samples were analyzed only for methane concentration. Groundwater samples were also collected from the active layer of the permafrost at the Barrow Environmental Observatory (BEO) inland from Elson Lagoon and the Beaufort Sea. River water samples were collected from creeks flowing into Kasitsna Bay and Elson Lagoon. Salinity and temperature were measured for all samples with a handheld YSI 85 multiprobe.

Radium activity

Large volume (80–230 L) seawater and river water samples were collected using either submersible pumps or buckets, while groundwater samples (volume 13–220 L) were collected using submersible pumps. Sample water was passed through a plastic column containing MnO_2^- impregnated acrylic fiber at a rate of <2 L min^{-1} for collection of Ra isotopes (Moore 2008). Samples were shipped to the University of California Santa Cruz for analysis on a Radium Delayed Coincidence Counter (RaDeCC) for measurement of ^{223}Ra and ^{224}Ra activities within less than 5 d (Moore and Arnold 1996). The fibers were analyzed on the RadeCC again 3-5 weeks after collection to correct for ^{228}Th supported ^{224}Ra, and 1 yr after collection for ^{228}Ra (Moore 2008; Young et al. 2008). Standards were run on a monthly basis as part of the quality control for maintenance of the instrument and analytical errors calculated using established methods (Garcia-Solsona et al. 2008). Units of these radium isotopes are most commonly denoted as disintegrations per minute (dpm) per volume of water (m^3).

Methane concentration

Discrete samples for methane analysis were collected in concert with each radium sample at both sites using methods previously described (Valentine et al. 2010). Additional samples for methane concentration analysis were collected from groundwater pits where not enough volume of water was obtainable for radium analysis. Methane concentration was also measured in the ocean water by means of an in situ survey, and methane flux to the atmosphere calculated as described in (Pierrot et al. 2009; Gülzow et al. 2011; Garcia-Tigreros Kodovska et al. unpubl.). In this context, an in situ survey refers to the measurement of methane by continuous sampling of water and immediate measurement of gases as described in Pierrot et al. 2009 with adaptation to methane instead of carbon dioxide.

Water isotopes

Water samples for δ^2H and δ^{18}O were collected by submersible pump in concert with the radium activity samples and filtered through 0.45 μm filters into 2 mL gas chromatography vials. Samples were analyzed by the UC Davis Stable Isotope Facility on a Laser Water Isotope Analyzer V2 (Los Gatos Research). Precision is typically ≤ 0.3 ‰ for δ^{18}O and ≤ 0.8 ‰ for δ^2H. Values are reported relative to Vienna Standard Mean Ocean Water (VSMOW). Water isotope samples were collected during 2012 only.

SGD flux calculations

SGD fluxes were calculated using the isotopes ^{223}Ra, ^{224}Ra, and ^{228}Ra and box-model equations modified from previous studies, which assume steady state conditions where sources on the left-hand side (LHS) balance sinks on the right-hand side (RHS) in Eqs. 1-3 (Hwang et al. 2005). SGD into the Beaufort Sea (Eqs. 1-3) was assumed to be the only source of radium to the coastal ocean, and advection and radioactive decay within the water column the only sinks.

$$Ra_{gw}^{223}G = Ra_{oce}^{223}V\lambda_{223} + \left(Ra_{oce}^{223} - Ra_{off}^{223}\right)V\tau \quad (1)$$

$$Ra_{gw}^{224}G = Ra_{oce}^{224}V\lambda_{224} + \left(Ra_{oce}^{224} - Ra_{off}^{224}\right)V\tau \quad (2)$$

$$Ra_{gw}^{228}G = Ra_{oce}^{228}V\lambda_{228} + \left(Ra_{oce}^{228} - Ra_{off}^{228}\right)V\tau \quad (3)$$

where Ra_{gw}^{223}, Ra_{gw}^{224}, and Ra_{gw}^{228} are the activities (dpm m^{-3}) of the respective isotopes in groundwater, Ra_{oce}^{223}, Ra_{oce}^{224}, and Ra_{oce}^{228} the activities (dpm m^{-3}) of the respective isotopes in the groundwater-influenced coastal ocean, Ra_{off}^{223}, Ra_{off}^{224}, and Ra_{off}^{228} are the offshore activities (dpm m^{-3}) of the respective isotopes, λ_{223}, λ_{224}, and λ_{228} are the decay constants (d^{-1}) of the respective isotopes, V is the volume (m^3) of the groundwater-influenced coastal ocean, and τ and G are unknown representing 1/residence time (d^{-1}) of the groundwater-influenced coastal ocean and the SGD flux (m^3 d^{-1}) to the coastal ocean, respectively. V was defined by the presence of excess radium in the coastal ocean, and depth of the water column where excess radium was observed.

A system of equations was similarly developed for Kasitsna Bay and Elson Lagoon. At Kastisna Bay and Elson Lagoon (Eqs. 4-6) river discharge and groundwater discharge were assumed to be sources of radium (due to the presence of rivers flowing into the bay and lagoon), and advection and radioactive decay were assumed to be the only sinks.

$$Ra_{gw}^{223}G + Ra_{riv}^{223}R = Ra_{oce}^{223}V\lambda_{223} + \left(Ra_{oce}^{223} - Ra_{off}^{223}\right)V\tau \quad (4)$$

$$Ra_{gw}^{224}G + Ra_{riv}^{224}R = Ra_{oce}^{224}V\lambda_{224} + \left(Ra_{oce}^{224} - Ra_{off}^{224}\right)V\tau \quad (5)$$

$$Ra_{gw}^{228}G + Ra_{riv}^{228}R = Ra_{oce}^{228}V\lambda_{224} + \left(Ra_{oce}^{228} - Ra_{off}^{228}\right)V\tau \quad (6)$$

where Ra_{riv}^{223}, Ra_{riv}^{224}, and Ra_{riv}^{228} are the activities (dpm m^{-3}) of the respective isotopes in river water entering the bay/lagoon, R is the river discharge (m^3 d^{-1}) entering the bay/lagoon and unknown, and all other terms are the same as in Eqs. 1-3. V was defined by the physical boundaries and depth of the bay/lagoon.

These systems of equations can be rearranged for unknowns (LHS) to balance knowns (RHS) and written linearly as

$$Ax = b \quad (7)$$

where A is a matrix of observed radium activities in the groundwater and river water (for Kasitsna Bay and Elson Lagoon), and excess radium activity in ocean water, x is a vector of unknown terms (G, R, and τ), and b is a vector of known terms (the radioactive decay of each isotope in the water column).

To fill the matrix A and vector b the distributions of the ocean and groundwater datasets for each site was determined using the chi-squared test for continuous distributions ($\alpha = 0.05$) against uniform, Gaussian, log-normal, and exponential distributions. Using information about the distribution of each dataset, and MATLAB pseudorandom number generators (syntax rand, randn, and exprnd), 1,000,000 artificial datasets were generated and solved for the unknown vector x. Nonreal solutions were avoided by adding negative signs to sink terms in matrix A, and forcing positive solutions using a nonnegative approach (MATLAB syntax lsqnonneg) (Lawson and Hanson 1974). Results for vector x were aggregated, with median computed.

Results

Water isotopes

$\delta^{18}O$ and $\delta^{2}H$ values relative to VSMOW for Kasitsna Bay (top panel) and the Beaufort Sea, Elson Lagoon, and BEO (bottom panel) are shown in Fig. 3. At Kasitsna Bay, the river water samples fall directly on the Global Meteoric Water Line (GMWL). Groundwater samples at Kasitsna Bay also lie relatively close to the GMWL. The groundwater samples lie between the river and ocean values.

Data for the Beaufort Sea are also on the GMWL, and are consistent with high-latitude ocean water (Schmidt 1998). Data from Elson Lagoon is consistently shifted to slightly more negative values on the GMWL than the Beaufort Sea and Kasitsna Bay. Samples collected from the active layer above the permafrost at the BEO are also slightly more negative along the GMWL. The tundra groundwater samples (e.g., water in the saturated zone of the active layer above the permafrost) lie to the right the GMWL, which is consistent with groundwater in arid regions where evaporation from the top of the water table is prevalent (Gat 1996). A best-fit line through the tundra groundwater data (Fig. 3 TG Fit) shows an intersection with the GMWL at values consistent with Siberian permafrost. Samples collected from the coastal STE of the Beaufort Sea generally lay between the Beaufort Sea values and the tundra groundwater values, trending closer to the Beaufort Sea values. However, a few of the Beaufort Sea coastal groundwater values are similar or even more negative in both isotopes than the tundra groundwater values. Similar results are observed for the Elson Lagoon coastal groundwater values, where the groundwater values tend to lie between the Elson Lagoon and tundra groundwater values, shifted towards the Elson Lagoon values.

A general shift is observed for all of the Elson Lagoon data (lagoon and groundwater) toward more negative (more permafrost influenced) values compared to all of the Beaufort Sea samples (seawater and groundwater), which are more similar to previously reported values for high latitude oceans. This shows that Elson Lagoon is more influenced by terrestrial waters than the Beaufort Sea.

Radium activities

Averages, ranges, and medians for ocean/lagoon water, coastal groundwater, BEO groundwater, and river water for ^{223}Ra, ^{224}Ra, and ^{228}Ra are shown in Table 1. ^{233}Ra, ^{224}Ra, and ^{228}Ra activities were consistently an order of magnitude

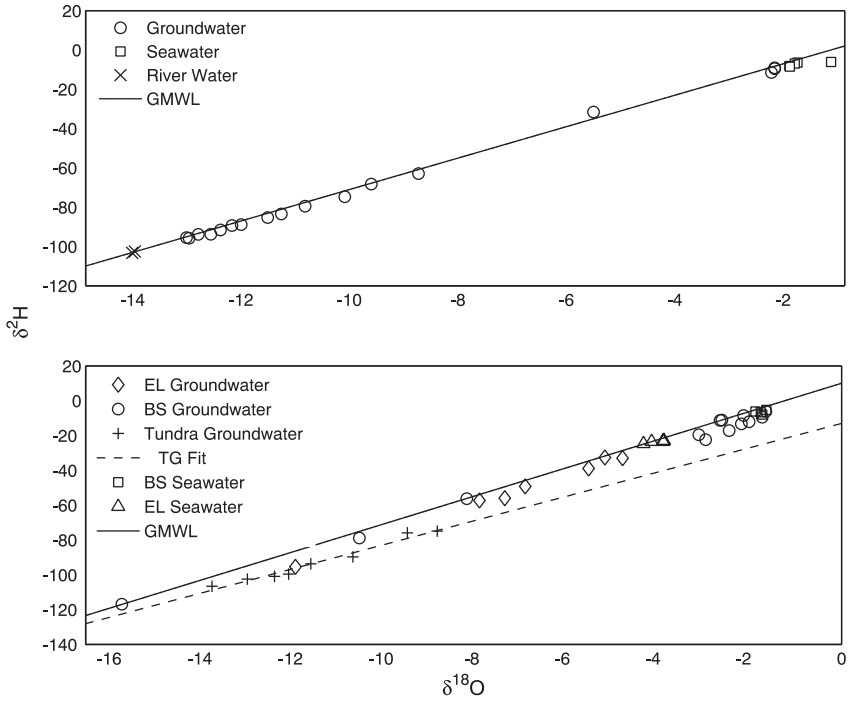

Fig. 3. Water isotope data relative to VSMOW for Kasitsna Bay (top panel) and the Beaufort Sea and Elson Lagoon (bottom panel). Kasitsna Bay shows quick infiltration of precipitation and simple mixing of groundwater and seawater. Beaufort Sea/Elson Lagoon shows groundwater on a mixing line with permafrost melt water and ocean water. Tundra groundwater also falls on a mixing line (TG fit, a best-fit line through the tundra groundwater data) between melt water and some unidentified water source, which is off set below the GMWL due to evaporation.

higher in groundwater than in ocean water at Kasitsna Bay (both 2011 and 2012), Elson Lagoon, and the Beaufort Sea. Ocean mean and median ^{223}Ra activities were consistent between 2011 (3.9 dpm m^{-3} and 1.8 dpm m^{-3}, respectively) and 2012 (2.1 dpm m^{-3} and 1.4 dpm m^{-3}, respectively), as were ^{224}Ra activities for 2011 (38.3 dpm m^{-3} and 22.3 dpm m^{-3}) and 2012 (39.4 dpm m^{-3} and 23.5 dpm m^{-3}). Ocean mean and median ^{228}Ra activities were higher in 2012 (23.5 dpm m^{-3} and 16.5 dpm m^{-3}) than 2011 (1.9 dpm m^{-3} and 1.7 dpm m^{-3}). However, this could be due to the lower number of samples in 2011 (17 compared to 43). River water ^{233}Ra, ^{224}Ra, and ^{228}Ra activities at Kasitsna Bay (both 2011 and 2012) and Elson Lagoon were lower than ocean water at their respective sites. Groundwater collected from the active layer above the permafrost at the BEO also had consistently lower ^{233}Ra, ^{224}Ra, and ^{228}Ra activities than groundwater collected closer to the Beaufort Sea and Elson Lagoon (in the temporary wells and pits at the coastline). This is due to the low salinity of these groundwater samples compare to those at the coastline, and is consistent with previously observed trends elsewhere (Moore and Krest 2004). Distributions were not calculated for river samples due to the low number of samples, but radium activities in the river samples were low. All end-members were either exponentially or log-normally distributed.

Groundwater fluxes

The volume of the bay/lagoon (V) in Eqs. 4-6 (Kasitsna Bay and Elson Lagoon) were constrained by the average depths (30 m and 1.5 m, respectively), and the surface area of Kasitsna Bay (2.25×10^6 m^2) and the area sampled in Elson Lagoon (4.55×10^7 m^2). V for the Beaufort Sea was determined by the presence of excess ^{224}Ra in transects extending perpendicular to shore (Fig. 4). ^{224}Ra is elevated close to shore in both transects, and decreases reaching a minimum at 1 km from shore. Activity increases again further from shore.

This increase is probably due to another source. Advection of high activity water from further south on the shore or east from Elson Lagoon, or the dissociation of gas hydrates or hydrocarbon seeps offshore (which has been correlated to higher radium activity) could account for this observation (Peterson et al. 2013; N. Dimova unpubl.). Because this offshore activity is likely not sourced from local groundwater we ignored it in our calculations and the offshore value was taken to be the lowest activity sample at this site, as observed in both transects in Fig. 4. V for Eqs. 1-3 (Beaufort Sea) was confined to 500 m (distance from shore of groundwater seepage) and the average depth within this area (2.5 m), and normalized to 1 m of shoreline.

Table 1. Mean and median (top row) and range and number of samples (bottom row) of radium activities (dpm m^{-3}), methane concentrations (nmol L^{-1}), and salinity.

	^{223}Ra	^{224}Ra	^{228}Ra	CH_4	Salinity
			Kasitsna Bay 2011		
Groundwater	13.0, 10.3	170.7, 144.7	3.6, 2.8	27.9, 26.3	18.4, 19.2
	(1.7–31.5) *n*=20	(26.7–323.9) *n*=20	(0.8–9.6) *n*=18	(8.1–44.4) *n*=9	(1.0–29.6) *n*=20
Private Wells				555, 110	0.3, 0.2
	3.9, 1.8	38.3, 22.3	1.9, 1.7	(23.7–2380) *n*=5	(0.2–0.6) *n*=5
Ocean Water	(0.4–22.3) *n*=32	(3.2–215.4) *n*=32	(0.7–4.5) *n*=17	32.7, 32.8	28.7, 29.6
	1.4, 1.1	20.3, 21.0	1.5, 1.6	(14.2–51.4) *n*=7	(17.1–30.2)*n*=32
River Water	(0.7–2.5) *n*=5	(8.5–22.0) *n*=5	(0.9–1.9) *n*=5	173, 32.8	11.6, 12.7
				(22.4–324) *n*=2	(0.1–27.3) *n*=5
			Kasitsna Bay 2012		
Groundwater	18.0, 10.8	297.9, 230.9	39.3, 27.9	33.4, 18.1	12.9, 8.0
	(1.7–73.3) *n*=21	(36.8–1213.1) *n*=21	(0.1–114.8) *n*=15	(0.0–103) *n*=22	(1.8–31.3) *n*=23
Ocean Water	2.1, 1.4	39.4, 23.5	23.5, 16.5	55.5, 32.0	30.6, 30.9
	(0.1–8.4) *n*=47	(0.8–416.5) *n*=47	(2.5–322.4) *n*=43	(3.7–112) *n*=46	(22.7–34.7)*n*=47
River Water	0.7, 0.5	8.3, 6.5	3.8, 3.3	59.7	4.7, 0.1
	(0.5–1.2) *n*=3	(5.2–13.1) *n*=3	(0.7–7.4) *n*=3	(22.7–96.6) *n*=4	(0.1–18.4) *n*=4
			Elson Lagoon 2012		
Groundwater	39.8, 31.3	1093.8, 948.7	377.2, 197.6	6770, 61.7	15.8, 17.4
	(5.7–103.4) *n*=9	(88.4–1176.6) *n*=9	(82.9–1548.6) *n*=8	(4.9–47,100) *n*=7	(1.0–24.6) *n*=10
Lagoon Water	20.2, 13.1	336.5, 218.1	152.0, 134.7	26.0, 19.3	25.5, 25.6
	(2.3–133.0) *n*=16	(10.9–1737.0) *n*=16	(104.4–273.2) *n*=12	(3.3–124) *n*=23	(23.8–26.8)*n*=16
River Water	13.1 *n*=1	277.9 *n*=1	174.3 *n*=1	19.3 *n*=1	26.5, *n*=1
			Beaufort Sea 2012		
Groundwater	71.6, 64.3	1230.3, 1050.4	267.1, 222.4	21.1, 19.7	15.8, 15.4
	(6.0–213.5) *n*=14	(89.8–3953.5) *n*=14	(57.8–685.5) *n*=14	(0.0–59.0) *n*=14	(2.5–29.5) *n*=15
Ocean Water	4.3, 1.7	80.2, 41.3	92.2, 61.2	40.6, 32.1	28.6, 29.9
	(0.0–57.0) *n*=45	(0.0–838.1) *n*=14	(15.7–1082.6) *n*=41	(0.0–251.0) *n*=69	(23.5–30.5)*n*=70
			Barrow Environmental Observatory 2012		
Groundwater	2.9, 2.2	108.2, 36.7	9.2, 5.4	36,600, 41,900	0.7, 0.2
	(0.3–6.6) *n*=5	(4.3–401.5) *n*=7	(4.3–18.0) *n*=3	(457–77,600) *n*=8	(0.1–4.4) *n*=9

Median values were chosen as representative of the SGD flux instead of the mean as the median was less susceptible to influence of anomalously high model runs, and the median values stabilized before the mean values. A well-known approximation of the standard error of the median is to multiply the standard error of the mean by 1.253, which is derived from the asymptotic variance formula (Rousseeuw and Christophe 1993). The standard error was calculated by dividing the standard deviation by the square root of the number of model runs. We calculated the error for the SGD fluxes in this fashion. SGD was not calculated for Kasitsna Bay 2011, because not enough data were available to determine the distributions of the end-members. However, the similar ^{223}Ra and ^{224}Ra activities in Kasitsna Bay implies a similar SGD flux for 2011, especially considering the dominant driving force of SGD at this site (tidal pumping) does not vary significantly year to year. Data for the 2 yr were not combined to calculate a flux because, when combined the distribution could not be determined. Fluxes are highest for Kasitsna Bay (120 ± 50 m^3 m^{-1} d^{-1}). The Beaufort Sea and Elson Lagoon have lower calculated fluxes (13.0 ± 0.2 m^3 m^{-1} d^{-1} and 12 ± 4 m^3 m^{-1} d^{-1}, respectively). These units reduce to m^{-2}, however, for clarity the units will continue to be displayed as m^3 m^{-1}, to act as a reminder that all fluxes are normalized to 1 m of shoreline.

Methane concentrations and fluxes

Averages, ranges, and medians for ocean/lagoon water, coastal groundwater, Kasitsna Bay private well groundwater, BEO groundwater, and river water for methane concentration are shown in Table 1. The highest mean and median methane concentrations (36,600 nmol L^{-1} and 41,900

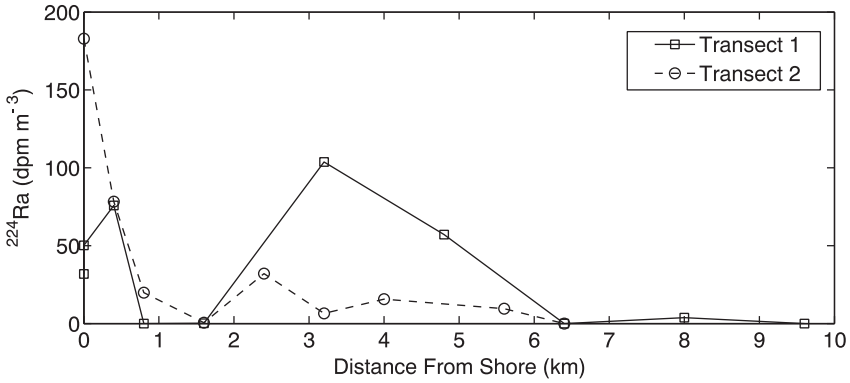

Fig. 4. ^{224}Ra activity in transects extending perpendicular from the coast in the Beaufort Sea. Elevated activity within 0.5 km of the shore is indicative of groundwater discharge. Elevated activity further offshore is likely due to another source and is not taken into account for calculations.

nmol L^{-1}) were observed in the groundwater of the BEO. This groundwater is in close contact with the actively thawing permafrost. Private well groundwater showed the highest methane concentrations at Kasitsna Bay (up to 2380 nmol L^{-1}). These wells are all fresh, with salinity < 1 and the groundwater is not influenced by the ocean.

Median and mean groundwater methane concentrations in the Beaufort Sea and Kasitsna Bay STE were similar (18.1 nmol L^{-1} to 33.4 nmol L^{-1}). Mean and median groundwater methane concentrations at Kasitsna Bay for 2011 (27.9 nmol L^{-1} and 26.3 nmol L^{-1}, respectively) are bounded by 2012 mean and median values (33.4 nmol L^{-1} and 18.1 nmol L^{-1}). Mean and median methane concentrations (6770 nmol L^{-1} and 61.7 nmol L^{-1}) in groundwater bordering Elson Lagoon are elevated above those observed at the Beaufort Sea and Kasitsna Bay coastal aquifers. However, these values are inflated by one extremely elevated sample (47,100 nmol L^{-1}) collected from an area where permafrost is in close contact with the lagoon. Medians, means, and ranges of methane concentration in seawater were similar for all the sites.

Methane fluxes were calculated by multiplying the median methane concentration of the coastal groundwater at each site by its respective SGD flux. The methane flux calculated in the Elson Lagoon is 11.8 ± 3.9 mg m^{-1} d^{-1}, due to the high median methane concentration in groundwater observed around Elson Lagoon. The highest observed groundwater methane concentration (47,100 nmol L^{-1}) along the coast of Elson Lagoon was where the coastline is dominated by permafrost, with the highest observed lagoon water methane concentration (124 nmol L^{-1}) measured in this area as well. The groundwater flow in this area is fresh and may, therefore, not be captured by the radium modeling method and is underrepresented in our calculations. The activity of ^{224}Ra of the high methane lagoon sample is an order of magnitude higher than all other samples along this coastline, which we believe to be indicative of groundwater discharge dominating at this site. This potential hotspot appears to be highly localized, as we did not observe any other lagoon sample with such high methane concentration. Therefore, our calculated methane flux, which used the median methane concentration is less affected by this high concentration sample (see Table 1 for mean and median methane concentrations of groundwater in Elson Lagoon), and is representative of the greater part of coastline in Elson lagoon apart from this hotspot.

Discussion

Kasitsna Bay

Water isotopes at Kasitsna Bay show a relatively simple hydrologic system (Fig. 3). River water samples so close to the GMWL (Gat 1996) indicate the source water to this river is primarily precipitation and runoff which has had little time to evaporate, while samples from the STE are also close to the GMWL, indicating quick infiltration into the STE. Samples from the STE lie on a mixing line between river and ocean samples, suggesting that groundwater in the STE is a mix between freshwater sourced from infiltration and seawater which has entered the STE. These data fall close to the ocean water end member indicating that the SGD is dominated by seawater (which is low in methane) which has recharged the STE by tidal and wave pumping, rather than fresh groundwater (which is high in methane) that is sourced from inland and driven mainly by hydraulic gradient. Under such settings, methane sourced from inland anoxic aquifers will be diluted by ocean water, yielding lower concentrations that decrease the SGD-associated methane flux. This is supported by the methane concentration data. At Kasitsna Bay the highest methane concentration groundwater had the lowest salinity, showing little ocean influence in those samples and a lower dilution ratio.

SGD volume fluxes are highest for Kasitsna Bay (120 ± 50 m^3 m^{-1} d^{-1}), which is consistent with the high tidal pumping effect, precipitation, and topographic relief

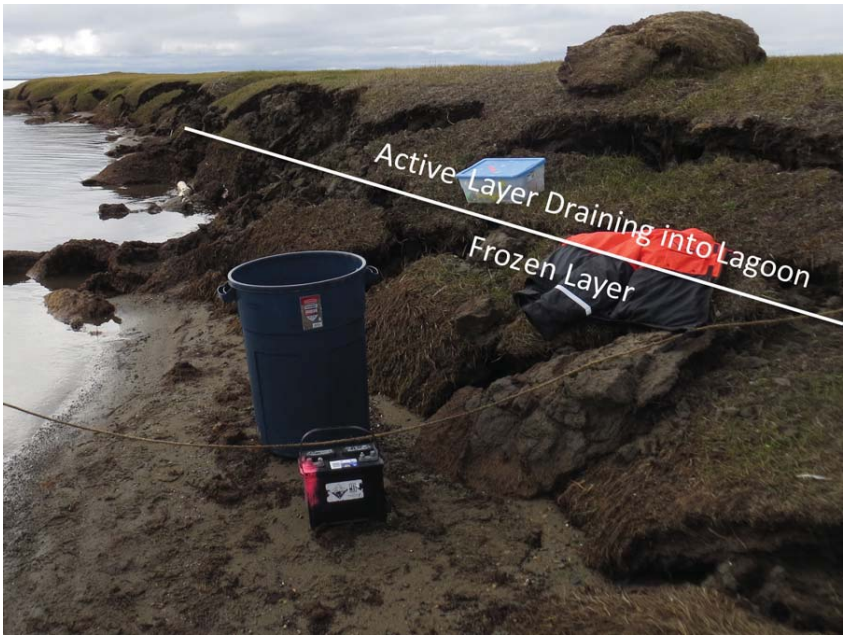

Fig. 5. Photograph of the southern shoreline of Elson Lagoon. The white line denotes the approximate boundary between the thawing active layer of the permafrost which discharges fresh groundwater into the lagoon, and the frozen permafrost below it.

present at this site. Likewise, the methane flux to Kasitsna Bay was highest at 35 ± 27 mg m^{-1} d^{-1} (based on 2011 data, although the similar bay radium activities and groundwater methane concentrations between 2011 and 2012 suggest a similar inter-annual flux). This is largely due to the high SGD volume flux at this site, as STE methane concentrations are similar to those at the Beaufort Sea.

Beaufort Sea and Elson Lagoon

Water isotopes at the more northern sites of our study, the Beaufort Sea and Elson Lagoon, show mixing characteristics similar to Kasitsna Bay (Fig. 3). Data from the STE generally show a mix between terrestrially sourced inland fresh groundwater from the active layer and seawater. However, unlike Kasitsna Bay fresh groundwater samples lie on a line to the right of the GMWL (TG fit), which is consistent with groundwater in arid regions, where evaporation from the top of the water table is prevalent (Gat 1996). The TG fit line shows an intersection with the GMWL at values consistent with Siberian permafrost, which suggests the source of this groundwater is permafrost melt (Sugimoto et al. 2003). A few samples ($n = 3$) collected from the Beaufort Sea STE display water isotopes similar to those from the active layer further inland (at the BEO), which may indicate hot spots of groundwater flow from the active layer to the ocean through the coastal gravel adjacent to the Beaufort Sea. However, this connection to the active layer does not appear to be present all along the coastline and most of the groundwater along the coast is of marine origin, as supported by the water isotope data. We cannot at this time determine what causes these preferential flow paths. They could be old river channels that have a thicker active layer depth, or a network of thermokarst features which cause depressions in the active layer. Thermokarst polygons are common in the BEO (Shiklomanov et al. 2010). More study is needed to fully understand this heterogeneity, but generally similar to Kasitsna Bay the presence of seawater in the STE of these sites will cause a diluting effect of high methane freshwater from the active layer by mixing with low methane seawater.

The Beaufort Sea and Elson Lagoon have lower calculated SGD volume fluxes (13.0 ± 0.2 m^3 m^{-1} d^{-1} and 12 ± 4 m^3 m^{-1} d^{-1}, respectively) than Kasitsna Bay, consistent with the low tidal pumping, topographic relief, and precipitation. All groundwater flowing into the Beaufort Sea in the area we sampled enters through a gravel beach where the fresh tundra water mixes with seawater, making the SGD brackish to saline in nature, which is easily traced using radium. However, in Elson Lagoon, brackish groundwater only discharges from the spit-bordered part of the lagoon. Much of Elson Lagoon (any part other than the spit) is bordered by permafrost, which in many places is elevated above the water level of the lagoon (Fig. 5). We surmise freshwater draining (dripping) from the active layer of the permafrost into the lagoon could constitute a substantial portion of groundwater discharge in this area; we have observed this process along much of the lagoon bordered by permafrost. Radium is not an effective tracer of

freshwater discharge in marine environments, and the portion of groundwater flow entering the lagoon from dripping from the active layer, which could be a substantial fraction of discharge into the lagoon, is not captured when using radium, making our SGD and SGD-associated methane fluxes an underestimate (Moore and Krest 2004).

As a result of the lower SGD volume fluxes, these sites have lower methane fluxes than Kasitsna Bay. The methane flux into the Beaufort Sea was lower than Elson Lagoon, with a flux of 4.1 ± 0.6 mg m^{-1} d^{-1} (compared to 11.8 ± 3.9 mg m^{-1} d^{-1} for Elson Lagoon) largely due to the median coastal groundwater methane concentration being one-third that of the Elson Lagoon value.

The groundwater sampled from the active layer of the BEO is in close contact with the actively thawing permafrost, and as a result these samples have high methane concentrations. Although somewhat disconnected from the ocean, groundwater similar to this mixes with seawater in the STE of the Beaufort Sea coastline, supplying methane to SGD on the coast. Groundwater directly from the active layer also drains (drips) into Elson Lagoon from the actively thawing permafrost that borders the lagoon (see Fig. 5). It is unclear how much methane degasses when groundwater drips from the active layer, and how much actually reaches the lagoon. While the close contact of the permafrost and lagoon water creates the potential for a high methane flux from the active layer to the lagoon, the methane flux is likely reduced due to the way the groundwater discharges from the active layer, potentially releasing methane directly into the atmosphere and not into the lagoon water. However, in a similar setting where the active layer above the permafrost is in direct contact with low energy coastal sites it is likely that the SGD associated methane fluxes will be higher.

Comparison of SGD volume fluxes to other studies

Radon-based groundwater discharge estimates were conducted in concert with this study (N. Dimova unpubl.). Radon-based estimates are in units of cm d^{-1}, and the conversions from the radium-based groundwater fluxes (m^3 m^{-1} d^{-1} or m^2 d^{-1}) to these units can be achieved by dividing the radium-derived groundwater flux by the area (m^2) of groundwater seepage (from *Groundwater Fluxes* in Results). For the Beaufort Sea, the seepage area is well defined by the presence of high ^{224}Ra activity in the seawater, and is the same as the surface area of the coastal box used in our model. This yields a radium-based specific discharge of 2.6 cm d^{-1}, which is similar to the radon-based flux (2.2 ± 0.5 cm d^{-1}). However, the radium-based specific discharges (calculated by multiplying the SGD times the length of the coastline of the bay and divided by the area of the bay) for Elson Lagoon (0.58 cm d^{-1}) and Kasitsna Bay (16 cm d^{-1}) are an order of magnitude less than those calculated using the Radon-based methods (2.1 ± 0.4 cm d^{-1} for Elson Lagoon and 186 ± 163 cm d^{-1} for Kasitsna Bay). This could result from a number of reasons.

A likely explanation is that radon accounts for the total groundwater discharge (brackish/saline and fresh) while radium only accounts for brackish/saline groundwater. Fresh groundwater discharge is particularly important in Elson Lagoon, where flow of water from the active layer at the cliff face bordering the lagoon, which is not in contact with seawater, could be substantial. Another cause of discrepancy is that the radon-mass balance did not account separately for river discharge but included it in the SGD flux, resulting in higher SGD fluxes while the radium-based calculations did make this correction. A previous study has also remarked that differences between radium and radon based SGD estimates can be due to heterogeneity in the STE that would affect the radon SGD end-member, resulting in differences between radium and radon based SGD estimates (Dulaiova et al. 2008). Indeed more samples were collected to constrain the radium SGD end-member than the radon SGD end-member. One more very likely possibility to explain the discrepancy is that the actual area of seepage is less than the area of the whole lagoon/bay. While this would not affect the radium-based groundwater fluxes, it does make the conversion between the two methods difficult and will result in discrepancies in the fluxes obtained from the different tracers. Dividing the radium-derived flux (m^3 m^{-1} d^{-1} or m^2 d^{-1}) by the radon-derived flux (cm d^{-1} or m d^{-1}) yields the distance from shore (m) the seepage face would need to be for the two tracers to be consistent. This yields a distance of 64 m for Kasitsna Bay, and 571 m for Elson Lagoon. Interestingly at Elson Lagoon this is similar to the distance from shore at the Beaufort Sea that is well defined by elevated ^{224}Ra activity (500 m).

Broader implications

Regional extrapolation of the methane fluxes presented here is beyond the scope of this study. However, our data from the two locations suggest that a similar range of fluxes may be expected throughout coastal Alaska. Understanding the governing factors controlling SGD associated methane flux to the oceans at each site is required prior to any attempt for extrapolation. Our data facilitates a first-order look into these governing factors.

With similar groundwater methane concentrations observed for both Kasitsna Bay and the Beaufort Sea, the difference in SGD associated methane flux is due primarily to the difference in SGD volume flux. The SGD volume flux at Kasitsna Bay (120 ± 50 m^3 m^{-1} d^{-1}) was an order of magnitude higher than at the Beaufort Sea (13.0 ± 0.2 m^3 m^{-1} d^{-1}), which is also consistent with the higher radon-based specific discharges at Kasitsna Bay (186 ± 163 cm s^{-1}) than the Beaufort Sea (2.2 ± 0.5 cm s^{-1}), (N. Dimova unpubl.), and the characteristics of each site that influence groundwater discharge, high tides, high topographic relief, and

high precipitation at Kasitsna Bay and low tides, low topographic relief, and low precipitation along the Beaufort Sea.

Higher groundwater methane concentrations were observed inland from the shores of Kasitsna Bay and the Beaufort Sea (up to 2,000 nmol L^{-1} and 78,000 nmol L^{-1}, respectively). However, Kasitsna Bay is more conducive to the transport of methane through SGD due to the areas physical characteristics. Furthermore, we postulate high precipitation combined with the high topographic relief likely begets a steep hydraulic gradient increasing groundwater flow rates and thus the transport of methane from inland groundwater to the coastal ocean at Kasitsna Bay.

The absence of a steep hydraulic gradient and the minimal wave/tidal pumping at the Beaufort Sea shoreline results in lower SGD associated methane flux, despite the very high methane concentrations observed in the groundwater of the active layer. Even if the methane flux at the Beaufort Sea site is multiplied by the entire coastline length of the Arctic Ocean (approximately 45,390 km) (Wright 2007), which exhibits a similar tidal range and degree of permafrost interaction, the total methane flux (6.79×10^{-5} Tg yr^{-1}) is a fraction of a percent of what is venting to the Arctic Ocean from sub-sea permafrost on the East Siberian shelf (approximately 7.89 Tg yr^{-1}) alone (Shakhova et al. 2010).

It is harder to extrapolate the methane fluxes at Kasitsna Bay, since the length of coastline within Alaska that has the same groundwater methane concentrations and SGD volume flux is impossible to constrain without more data. However, we do speculate that SGD-associated methane flux to the Pacific Ocean, which has fewer other sources of methane, (e.g., no subsea permafrost) than the Arctic Ocean, could be a substantial source of methane to the Pacific, especially in near-shore areas. To put into context the SGD associated methane fluxes at the Kasitsna Bay site, we calculated the distance from shore for which the sea to air methane fluxes could be solely supported by SGD.

The average sea to air methane flux at Kasitsna Bay is 0.5 ± 0.42 μmol (0.008 mg) m^{-2} d^{-1} (Kodovska et al. unpubl.). Dividing the SGD associated methane flux by the sea to air methane flux yields the distance from shore the sea to air methane flux could be supported by SGD alone; this distance is 4.4 km. This calculation represents a maximum estimate where there exist no sinks of methane in the water column. Our calculation highlights the potential importance of SGD as a source of methane to the coastal north Pacific. Additional studies are needed to determine if the SGD-associated methane fluxes at Kasitsna Bay are representative of other similar northern-Pacific coastlines and to determine the relative importance of SGD to methane in the water column relative to other sources. Fluxes to the Bering Sea, the coastline of which was not analyzed in this study, should also be estimated. These data would help to constrain a global flux of methane through this process to both the world ocean and the atmosphere.

References

Archer, D., B. Buffett, and V. Brovkin. 2009. Ocean methane hydrates as a slow tipping point in the global carbon cycle. Proc. Natl. Acad. Sci. USA **106**: 20596–20601. doi: 10.1073/pnas.0800885105

Boucher, T. V., and B. R. Mead. 2006. Vegetation change and forest regeneration on the Kenai Peninsula, Alaska following a spruce beetle outbreak, 1987-2000. For. Ecol. Manage. **227**: 233–246. doi:10.1016/j.foreco.2006.07.001

Brown, J., O. J. Ferrians, J. A. Heginbottom, and E. S. Melnikov. 2001. Circum-arctic map of permafrost and ground ice conditions. National Snow and Ice Data Center.

Bugna, G. C., J. P. Chanton, J. E. Cable, W. C. Burnett, and P. H. Cable. 1996. The importance of groundwater discharge to the methane budgets of nearshore and continental shelf waters of the northeastern Gulf of Mexico. Geochim. Cosmochim. Acta **60**: 4735–4746. doi:10.1016/S0016-7037(96)00290-6

Cable, J. E., G. C. Bugna, W. C. Burnett, and J. P. Chanton. 1996. Application of 222Rn and CH4 for assessment of groundwater discharge to the coastal ocean. Limnol. Oceanogr. **41**: 1347–1353. doi:10.4319/lo.1996.41.6.1347

Dulaiova, H., R. Camilli, P. B. Henderson, and M. A. Charette. 2010. Coupled radon, methane and nitrate sensors for large-scale assessment of groundwater discharge and non-point source pollution to coastal waters. J. Environ. Radioact. **101**: 553–563. doi:10.1016/j.jenvrad.2009.12.004

Dulaiova, H., M. E. Gonneea, P. B. Henderson, and M. A. Charette. 2008. Geochemical and physical sources of radon variation in a subterranean estuary—implications for groundwater radon activities in submarine groundwater discharge studies. Mar. Chem. **110**: 120–127. doi: 10.1016/j.marchem.2008.02.011

Flores, R. M., and G. D. Stricker. 1992. Reservoir framework architecture in the Clamgulchian type section (pliocene) of the sterling formation, Kenai Peninsula, Alaska. U.S Geol. Surv. Bull. **2068**: 118–129.

Garcia-Solsona, E., J. Garcia-Orellana, P. Masqué, and H. Dulaiova. 2008. Uncertainties associated with 223Ra and 224Ra measurements in water via a Delayed Coincidence Counter (RaDeCC). Mar. Chem. **109**: 198–219. doi: 10.1016/j.marchem.2007.11.006

Gat, J. R. 1996. Oxygen and hydrogen isotopes in the hydrologic Cycle. Annu. Rev. Earth Planet. Sci. **24**: 225–262. doi:10.1146/annurev.earth.24.1.225

Gülzow, W., G. Rehder, B. Schneider, J. S. v. Deimling, and B. Sadkowiak. 2011. A new method for continuous measurement of methane and carbon dioxide in surface waters using off-axis integrated cavity output spectroscopy (ICOS): An example from the Baltic Sea. Limnol.

Oceanogr.: Methods **9**: 176–184. doi:10.4319/lom.2011.9.176

Hinkel, K. M., and F. E. Nelson. 2003. Spatial and temporal patterns of active layer thickness at Circumpolar Active Layer Monitoring (CALM) sites in northern Alaska, 1995-2000. J. Geophys. Res. **108**. doi:10.1029/2001JD000927

Hovland, M., A. G. Judd, and R. A. Burke. 1993. The global flux of methane from shallow submarine sediments. Chemosphere **26**: 559–578. doi:10.1016/0045-6535(93)90442-8

Hwang, D.-W., G. Kim, Y.-W. Lee, and H.-S. Yang. 2005. Estimating submarine inputs of groundwater and nutrients to a coastal bay using radium isotopes. Mar. Chem. **96**: 61–71. doi:10.1016/j.marchem.2004.11.002

Kitidis, V., R. C. Upstill-Goddard, and L. G. Anderson. 2010. Methane and nitrous oxide in surface water along the North-West Passage, Arctic Ocean. Mar. Chem. **121**: 80–86. doi:10.1016/j.marchem.2010.03.006

Knee, K., and A. Paytan. 2011. 4.08 Submarine groundwater discharge: A source of nutrients, metals, and pollutants to the coastal ocean. Treatise Estuar. Coast. Sci. **4**: 205–234. doi:10.1016/B978-0-12-374711-2.00410-1

Lawson, C. L., and R. J. Hanson. 1974. Solving least Squares Problems, pp. 340, Prentice-Hall Englewood Cliffs, N.J., 1974, Society for Industrial and Applied Mathematics.

Moore, W. 1996. Using the radium quartet for evaluating groundwater input and water exchange in salt marshes. Geochim. Cosmochim. Acta **60**: 4645–4652. doi:10.1016/S0016-7037(96)00289-X

Moore, W., and R. Arnold. 1996. Measurement of 223Ra and 224Ra in coastal waters using a delayed coincidence counter. J. Geophys. Res.: Oceans **101**: 1321–1329. doi:10.1029/95JC03139

Moore, W. S. 1999. The subterranean estuary: A reaction zone of ground water and sea water. Mar. Chem. **65**: 111–125. doi:10.1016/S0304-4203(99)00014-6

Moore, W. S. 2008. Fifteen years experience in measuring 224Ra and 223Ra by delayed-coincidence counting. Mar. Chem. **109**: 188–197. doi:10.1016/j.marchem.2007.06.015

Moore, W. S., and J. Krest. 2004. Distribution of 223Ra and 224Ra in the plumes of the Mississippi and Atchafalaya Rivers and the Gulf of Mexico. Mar. Chem. **86**: 105–119. doi:10.1016/j.marchem.2003.10.001

Munroe, J. S., and others. 2007. Application of ground-penetrating radar imagery for three-dimensional visualisation of near-surface structures in ice-rich permafrost, Barrow, Alaska Permafrost Periglacial Process. **18**: 309–321. doi:10.1002/ppp.594

Overduin, P. P., S. Westermann, K. Yoshikawa, T. Haberlau, V. Romanovsky, and S. Wetterich. 2012. Geoelectric observations of the degradation of nearshore submarine permafrost at Barrow (Alaskan Beaufort Sea). J. Geophys. Res. **117**: F02004. doi:10.1029/2011JF002088

Paytan, A., and others. 2015. Methane transport from the active layer to lakes in the Arctic using Toolik Lake, Alaska, as a case study. Proc. Natl. Acad. Sci. USA 201417392. doi:10.1073/pnas.1417392112

Peterson, R. N., R. F. Viso, I. R. MacDonald, and S. B. Joye. 2013. On the utility of radium isotopes as tracers of hydrocarbon discharge. Mar. Chem. **156**: 98–107. doi:10.1016/j.marchem.2013.02.008

Pierrot, D., and others. 2009. Recommendations for autonomous underway pCO2 measuring systems and data-reduction routines. Deep-Sea Res. Part II Top. Stud. Oceanogr. **56**: 512–522. doi:10.1016/j.dsr2.2008.12.0

Rousseeuw, P. J., and C. Christophe. 1993. Alternatives to the median absolute deviation. J. Am. Stat. Assoc. **88**: 1273–1283.

Schmidt, G. A. 1998. Oxygen-18 variations in a global ocean model. Geophys. Res. Lett. **25**: 1201–1204. doi:10.1029/98GL50866

Shakhova, N., and I. Semiletov. 2007. Methane release and coastal environment in the East Siberian Arctic shelf. J. Mar. Syst. **66**: 227–243. doi:10.1016/j.jmarsys.2006.06.006

Shakhova, N., I. Semiletov, A. Salyuk, V. Yusupov, D. Kosmach, and O. Gustafsson. 2010. Extensive methane venting to the atmosphere from sediments of the East Siberian Arctic Shelf. Science **327**: 1246–1250. doi:10.1126/science.1182221

Shakhova, N. E., V. I. Sergienko, and I. P. Semiletov. 2009. The contribution of the East Siberian shelf to the modern methane cycle. Her. Russ. Acad. Sci. **79**: 237–246. doi:10.1134/S101933160903006X

Shiklomanov, N. I., and others. 2010. Decadal variations of active-layer thickness in moisture-controlled landscapes, Barrow, Alaska. J. Geophys. Res. Biogeosci. **115**. doi:10.1029/2009JG001248

Stafford, J. M., G. Wendler, and J. Curtis. 2000. Temperature and precipitation of Alaska: 50 year trend analysis. Theor. Appl. Climatol. **67**: 33–44. doi:10.1007/s007040070014

Sugimoto, A., and others. 2003. Characteristics of soil moisture in permafrost observed in East Siberian taiga with stable isotopes of water. Hydrol. Process. **17**: 1073–1092. doi:10.1002/hyp.1180

Valentine, D. L., and others. 2010. Propane respiration jump-starts microbial response to a deep oil spill. Science **330**: 208–211. doi:10.1126/science.1196830

Wright, J. W. 2007. The New York Times Almanac 2007: The Alamanac of Record. In J.W. Wright [ed.]. Penguin Books.

Young, M. B., M. E. Gonneea, D. A. Fong, W. S. Moore, J. Herrera-Silveira, and A. Paytan. 2008. Characterizing

sources of groundwater to a tropical coastal lagoon in a karstic area using radium isotopes and water chemistry. Mar. Chem. **109**: 377–394. doi:10.1016/j.marchem.2007.07.010

Zimov, S., E. Schuur, and F. Chapin, III. 2006. Permafrost and the global carbon budget. Science(Washington) **312**: 1612–1613. doi:10.1126/science.1128908

Acknowledgments

We would like to thank Ryan Harmon, Mimi Peterson, and Tyler Sproule for their assistance in receiving and analyzing the radium samples in Santa Cruz, while the rest of the research team was in the field. This project was funded by NSF-OPP grant ARC 1114485 to AP and ST and NSF OCE-1139203 to JK. Scientific and technical support was provided by the NOAA and UAF Kasitsna Bay Laboratory, Naval Arctic Research Laboratory, and NSF Polar Field Services.

Submitted 29 August 2014
Revised 20 January 2015; 30 April 2015
Accepted 1 May 2015

Associate editor: Mary Scranton